

# Coupled Rotor/Fuselage Vibration Analysis for a Teetering Rotor and Comparison with Flight Test Data

Hyeonsoo Yeo\*

Inderjit Chopra†

Alfred Gessow Rotorcraft Center  
Department of Aerospace Engineering  
University of Maryland, College Park, MD 20742

## Abstract

A comprehensive vibration analysis of a coupled rotor/fuselage system for a two-bladed teetering rotor using finite element methods in space and time is developed that incorporate consistent rotor/fuselage structural, aerodynamic and inertial couplings and a modern free wake model. Coupled nonlinear periodic blade and fuselage equations are transformed to the modal space in the fixed frame and solved simultaneously. The elastic line airframe model of the AH-1G helicopter from the DAMVIBS program is integrated into the elastic rotor finite element model. Analytical predictions of rotor controls, blade loads and vibration are compared with flight test data. Predicted rotor control angles, blade torsional, and chord bending moments show relatively good agreement with test data. Blade beam bending moments overpredicts test measurements and needs further investigation. Calculated 2/rev and 4/rev vertical vibration levels at pilot seat show good correlation with the flight test, but predicted lateral vibration levels are much higher than measurements particularly at high advance ratios. In future, parametric studies will be carried out to investigate the sensitivity of different design parameters and modeling refinements on the prediction of blade loads and vibration.

## Nomenclature

$R$	rotor radius
$c$	blade chord
$\Omega_0$	reference rotor speed

\* Graduate Research Assistant

† Minter-Martin Professor and Director

Presented at the 23rd European Rotorcraft Forum, 16-18 September 1997, Dresden, Germany

$m$	blade mass per unit length
$m_0$	reference mass per unit length
$\sigma$	rotor solidity ratio
$C_T$	rotor thrust coefficient
$EI_y$	blade flap bending stiffness
$EI_z$	blade lag bending stiffness
$EA$	blade axial stiffness
$GJ$	blade torsional stiffness
$k_{m_1}, k_{m_2}$	radius of gyrations
$u, v, w$	blade elastic displacements in the axial, lag and flap directions
$\hat{\phi}$	blade elastic twist
$h$	shaft height
$\dot{x}_f, \dot{y}_f, \dot{z}_f$	fuselage translational velocities in global directions
$\ddot{x}_f, \ddot{y}_f, \ddot{z}_f$	fuselage translational accelerations in global directions
$\dot{\alpha}_s, \dot{\phi}_s, \dot{\psi}_s$	fuselage pitch, roll, and yaw rates
$\ddot{\alpha}_s, \ddot{\phi}_s, \ddot{\psi}_s$	fuselage pitch, roll, and yaw accelerations

## Introduction

Helicopters are susceptible to excessive vibration because of the nonsteady aerodynamic environment at the rotor disk, nonlinear inertial couplings of slender rotating blades, and complex rotor-fuselage interactional effects. A high level of vibration causes failure fatigue of components and human discomfort, seriously affects ride quality and system reliability, increases maintenance costs and degrades equipment performance. Therefore, design of a helicopter with inherently low vibration is an important goal, and for this, prediction of vibration at an early design stage is essential. Even though there has been enormous progress with vibration suppression technology, weight penalty has been excessive in part because of inadequate prediction methodology.

During the last two decades, coupled rotor-fuselage vibration analyses have been developed by many researchers using a variety of assumptions and solution methods. (see reviews by Reichert [1], Loewy [2] and Kvaternik, et al. [3]) They all emphasized the importance of understanding the fully coupled aeroelastic behavior of a rotor-fuselage system under different flight conditions.

Staley and Sciarra [4] used an explicit impedance matching technique for a linear coupled rotor-fuselage analysis in forward flight. The method was used for the vibration prediction of the Model 347 helicopter. Only the vertical hub motion was coupled to the lumped parameter rotor model undergoing flap and torsion motion, and vertical hub forces were calculated using the force summation method. Airframe dynamics was represented in terms of mobility matrix obtained from either analytical models or airframe shake tests. Vibratory hub loads were determined using hub-fixed conditions plus a correction factor due to hub motion. Correlation of predicted cockpit vibration levels with flight test data (Model 347) was found to be less than satisfactory.

Simplified investigations such as those reported in References [5-7] have made significant contributions to the understanding of the basic characteristics of rotorcraft vibration but are not sufficient for accurate predictions. The impedance matching method was often used to determine the vibration of a fuselage with a simple rotor model and highly simplified aerodynamics. For example, Hohnemeser and Yin [5] performed a coupled rotor/support analysis. The rotor blade was assumed to undergo only flapping motion and the body was modeled as concentrated inertias and support springs. The rotor impedances were computed directly with a finite element method that includes aerodynamics. The method was limited to hovering flight. They concluded that the excitation of the airframe with the rotor forces calculated using a hub-fixed condition can lead to large errors in the vibratory response. Hsu and Peters [6] calculated rotor impedance using blade flap motion only for a wide range of rotor parameters. Fuselage impedance was calculated by assuming it as a uniform beam with three rigid-body modes, representing respectively plunge, roll and pitch motions. They showed that the hub motion has a considerable influence on the hub loads for a relatively stiff rotor and the hover approximation for the calculation of rotor impedance is inadequate. Kunz [7] carried out a parametric study for a fully coupled vibration model consisting of a rotor with flapping degree of

freedom plus pylon and fuselage pitching motion. Fuselage response and hub loads were calculated using a harmonic balance method in conjunction with the impedance matching method. It was concluded that there is a potential for reducing vibratory response through the change of the blade structural parameters.

Using a finite element analysis, Rutkowski [8] investigated dynamic coupling between the rotor and the fuselage in hover analytically. Only vertical bending motion was considered in the finite element model of rotor as well as fuselage. Again, this study showed the importance of hub motion in the calculation of rotor response and resulting hub loads. Gabel and Sankewitsch [9] presented a coupling of the fuselage and rotor impedance matrix equations. A rotor impedance matrix was developed using the C60 rotor code, and a fuselage impedance matrix was obtained from a shake test as well as from a finite element analysis. Parametric studies were performed for a wind tunnel model with five degrees of freedom (vertical, lateral, longitudinal, roll, and pitch) hub motions. The importance of rotor-body coupling was demonstrated by showing that results with coupling differ significantly from those obtained with coupling neglected. Because the above analyses were based mostly on either simple rotor blade models or very idealized fuselage models using quasisteady aerodynamics and uniform inflow distribution, they yielded only qualitative trends.

It is now well established that nonlinear blade forces contribute significantly to vibratory hub loads. Thus, a consistent set of nonlinear coupled equations of motion of elastic rotor-fuselage is essential in the prediction of vibration. Warmbrodt and Friedmann [10] and Bir and Chopra [11] derived such equations for an elastic rotor coupled with six rigid body motion of a fuselage.

Vellaichamy and Chopra [12] presented a coupled rotor-fuselage analysis using elastic blade and flexible fuselage modeling (stick model). A finite element method in time was used to solve blade steady response, and a harmonic balance method was used to calculate body response due to periodic hub forcing. Rotor-body coupling was achieved using an iterative procedure. They emphasized the role of rotor-fuselage coupling and the importance of detailed modelings of rotor and fuselage. Chiu and Friedmann [13] developed a coupled elastic rotor/elastic fuselage model for vibration reduction studies. A collection of elements (beam, truss and plate) was

suggested to model three-dimensional fuselage. The coupled elastic blade equations, elastic and rigid fuselage equations, and the overall vehicle trim equations were solved using a harmonic balance technique. Later the active control of structural response(ACSR) scheme was applied to their model to minimize fuselage vibration [14]. They too pointed out the importance of nonlinear couplings and flexibility of the fuselage in the prediction of vibration.

Most analyses incorporated highly idealized aerodynamics. Helicopter vibration is due to the higher harmonic airloading of the rotor, thus nonuniform induced velocities caused by blade vortices can be a key element in the prediction of vibration. Yeo and Chopra [15] presented a coupled rotor/fuselage analysis using finite element methods in space and time. The elastic line model of the AH-1G helicopter in conjunction with an 4-bladed elastic hingeless rotor was used in the analysis. For the calculation of inflow and blade loads, a pseudo-implicit free wake model [16] and time-domain unsteady aerodynamics [17] were incorporated. The importance of rotor/fuselage coupling effects, refined aerodynamic modeling, and fuselage flexibility was addressed.

NASA-Langley carried out a successful Design Analysis Methods for Vibrations(DAMVIBS) program to establish the technology for accurate and reliable vibration prediction capability during the design of a rotorcraft. Four major helicopter manufacturers(Bell, Boeing, McDonnell Douglas, and Sikorsky) actively participated in this program. Systematic modeling and analysis techniques were investigated, including airframe finite element modeling, modeling refinements for difficult components, coupled rotor-airframe vibration analysis, and airframe structural optimization. They developed state-of-the-art finite element models for the airframe, conducted ground vibration tests, and made test/analysis comparisons. Under the DAMVIBS program, the four helicopter companies also applied their own methods to calculate the vibrations of the AH-1G helicopter, and correlated the predictions with an Operational Load Survey(OLS) flight test data. They identified modeling requirements for the vibration analysis of complex helicopter structures and rotor-fuselage coupling effects. Most of the analyses were unable to predict vibration accurately for all flight conditions.

This paper develops a comprehensive vibration analysis of a coupled rotor/fuselage system for a two-bladed teetering rotor using finite element methods in space and time, incorporating

consistent rotor/fuselage structural, aerodynamic, and inertial couplings and a modern free wake model. The elastic line model of the AH-1G helicopter from DAMVIBS program is integrated with the two bladed teetering elastic rotor finite element model. Vibration levels are calculated at several different flight conditions and validated with the flight test data.

## Formulation and Solution Procedure

The baseline rotor analysis is taken from UMARC where each blade is assumed to be an elastic beam undergoing flap and lag bending, elastic twist and axial deflection. The analysis for a two-bladed teetering rotor is formulated and incorporated into UMARC. The elastic rotor coupled equations include six hub degrees of motion. The airframe is discretized into beam elements, each undergoing vertical and lateral bending, elastic twist and axial deformation. The rotor vibratory loads are transmitted to the fuselage through the hub and the effects of fuselage motion are included in the determination of blade loads.

The derivation of the coupled rotor/fuselage equations of motion are based on Hamilton's variational principle generalized for a nonconservative system. It can be expressed as

$$\delta\Pi = \int_{t_1}^{t_2} (\delta U - \delta T - \delta W) dt = 0 \quad (1)$$

where  $\delta U$  is the virtual variation of strain energy,  $\delta T$  is the virtual variation of kinetic energy, and  $\delta W$  is the virtual work done by external forces. These virtual variations take into consideration contributions from both the rotor and the fuselage.

$$\delta U = \delta U_R + \delta U_F = \left( \sum_{b=1}^{N_b=1} \delta U_b \right) + \delta U_F \quad (2)$$

$$\delta T = \delta T_R + \delta T_F = \left( \sum_{b=1}^{N_b=1} \delta T_b \right) + \delta T_F \quad (3)$$

$$\delta W = \delta W_R + \delta W_F = \left( \sum_{b=1}^{N_b=1} \delta W_b \right) + \delta W_F \quad (4)$$

where the subscripts b and F refer to the blade and fuselage respectively and  $N_b$  is the total number of rotor blades.

## Coordinate Systems

Coordinate systems to model the teetering rotor is shown in Fig. 1 The transformation between

the inertial system and the hub-fixed nonrotating system is defined as

$$\begin{Bmatrix} \hat{I}_H \\ \hat{J}_H \\ \hat{K}_H \end{Bmatrix} = \begin{bmatrix} 1 & 0 & \alpha_s \\ 0 & 1 & -\phi_s \\ -\alpha_s & \phi_s & 1 \end{bmatrix} \begin{Bmatrix} \hat{I}_I \\ \hat{J}_I \\ \hat{K}_I \end{Bmatrix} \quad (5)$$

where  $\alpha_s$  and  $\phi_s$  are longitudinal and lateral shaft tilt angles respectively. The transformation between the hub-fixed nonrotating and rotating systems is defined as

$$\begin{Bmatrix} \hat{I} \\ \hat{J} \\ \hat{K} \end{Bmatrix} = \begin{bmatrix} \cos \psi & \sin \psi & 0 \\ -\sin \psi & \cos \psi & 0 \\ 0 & 0 & 1 \end{bmatrix} \begin{Bmatrix} \hat{I}_H \\ \hat{J}_H \\ \hat{K}_H \end{Bmatrix} \quad (6)$$

The coordinate transformation between the hub-fixed rotating system and the undeformed blade coordinate system is given by

$$\begin{Bmatrix} \hat{i} \\ \hat{j} \\ \hat{k} \end{Bmatrix} = \begin{bmatrix} \cos(\beta_p + \beta_T) & 0 & \sin(\beta_p + \beta_T) \\ 0 & 1 & 0 \\ -\sin(\beta_p + \beta_T) & 0 & \cos(\beta_p + \beta_T) \end{bmatrix} \begin{Bmatrix} \hat{I} \\ \hat{J} \\ \hat{K} \end{Bmatrix} \quad (7)$$

where  $\beta_T = \beta_G(-1)^m$  is a teetering angle for  $m^{\text{th}}$  blade and  $\beta_p$  is a precone angle.

The above transformation matrices are used to obtain blade velocities and accelerations for calculation of the aerodynamic loads and kinetic energy.

### Kinetic Energy

To derive the kinetic energy expression for the blade, we need the blade velocity in the deformed frame. This velocity consists of blade motion relative to the hub and the motion of the hub itself. This relation is expressed as

$$\vec{V} = \vec{V}_b + \vec{V}_f \quad (8)$$

where  $\vec{V}_b$  is the velocity of the blade relative to the hub and  $\vec{V}_f$  is the velocity of the blade induced by the motion of the fuselage. The velocity at point P on the blade is

$$\vec{V} = \dot{x}_1 \hat{i} + \dot{y}_1 \hat{j} + \dot{z}_1 \hat{k} + \vec{\omega}_b \times \vec{r}_b + \vec{\omega}_f \times \vec{r}_h + \dot{x}_F \hat{I}_I^G + \dot{y}_F \hat{J}_I^G + \dot{z}_F \hat{K}_I^G \quad (9)$$

where

$$\vec{r}_b = x_1 \hat{i} + y_1 \hat{j} + z_1 \hat{k} \quad (10)$$

$$\vec{r}_h = x_{CG} \hat{I}_F + y_{CG} \hat{J}_F + h \hat{K}_F \quad (11)$$

$$\vec{\omega}_b = -\dot{\phi}_s \hat{I}_I - \dot{\alpha}_s \hat{J}_I + \dot{\psi}_s \hat{K}_I + \Omega \hat{K}_H - \dot{\beta}_T \hat{J}_I \quad (12)$$

$$\vec{\omega}_f = -\dot{\phi}_s \hat{I}_I - \dot{\alpha}_s \hat{J}_I + \dot{\psi}_s \hat{K}_I \quad (13)$$

The  $\dot{\alpha}_s$ ,  $\dot{\phi}_s$  and  $\dot{\psi}_s$  are fuselage pitch, roll and yaw rates and  $\dot{x}_F$ ,  $\dot{y}_F$  and  $\dot{z}_F$  are fuselage longitudinal, lateral and vertical velocities. The velocity is expressed in the deformed frame as follows

$$\begin{aligned} \vec{V} &= V_x \hat{i} + V_y \hat{j} + V_z \hat{k} \\ &= (V_{bx} + V_{fx}) \hat{i} + (V_{by} + V_{fy}) \hat{j} \\ &\quad + (V_{bz} + V_{fz}) \hat{k} \end{aligned} \quad (14)$$

where

$$V_{bx} = \dot{x}_1 - y_1 \cos(\beta_p + \beta_T) - z_1 \dot{\beta}_T \quad (15)$$

$$V_{fx} = (\dot{x}_F - h \dot{\alpha}_s - y_{CG} \dot{\psi}_s) \cos \psi + (\dot{y}_F + h \dot{\phi}_s + x_{CG} \dot{\psi}_s) \sin \psi \quad (16)$$

$$V_{by} = \dot{y}_1 - x_1 \cos(\beta_p + \beta_T) - z_1 \sin(\beta_p + \beta_T) \quad (17)$$

$$V_{fy} = -(\dot{x}_F - h \dot{\alpha}_s - y_{CG} \dot{\psi}_s) \sin \psi + (\dot{y}_F + h \dot{\phi}_s + x_{CG} \dot{\psi}_s) \cos \psi + x \dot{\psi}_s \quad (18)$$

$$V_{bz} = \dot{z}_1 + x_1 \dot{\beta}_T + y_1 \sin(\beta_p + \beta_T) \quad (19)$$

$$V_{fz} = \dot{z}_F + x \dot{\alpha}_s \cos \psi - x \dot{\phi}_s \sin \psi + x_{CG} \dot{\alpha}_s - y_{CG} \dot{\phi}_s \quad (20)$$

### Air Velocity Components

The incident velocity at a particular blade station consists of three components; the flight velocity, the blade velocity and the velocity induced by fuselage motion. The general expression for the resultant blade velocity at a radial station  $x$  in the rotating undeformed frame is

$$\vec{V} = -\vec{V}_w + \vec{V}_b + \vec{V}_f \quad (21)$$

where  $\vec{V}_w$  is the flight velocity with contributions from the vehicle forward speed and the rotor inflow,  $\vec{V}_b$  is the blade velocity relative to the hub fixed frame resulting from blade rotation and blade motions and  $\vec{V}_f$  is the blade velocity due to fuselage motion.

The teetering motion induced blade velocity (at point  $P_{\eta_r}$  at three quarter chord on the rotating

deformed blade) is given by

$$\frac{U_R}{\Omega R} = -\omega\dot{\beta}_T - \eta_r \sin \theta_0 \dot{\beta}_T + \omega' x \dot{\beta}_T + \lambda \beta_T + \mu \omega' \beta_T \cos \psi + \mu \beta_p \beta_T \cos \psi \quad (22)$$

$$\frac{U_T}{\Omega R} = -\omega \beta_T \cos \theta_0 - x \beta_p \beta_T \cos \theta_0 + x \dot{\beta}_T \sin \theta_0 + \dot{\phi} x \dot{\beta}_T \cos \theta_0 + v \beta_T \sin \theta_0 + \mu \beta_T \sin \theta_0 \cos \psi + \mu \beta_T \dot{\phi} \cos \theta_0 \cos \psi \quad (23)$$

$$\frac{U_P}{\Omega R} = \omega \beta_T \sin \theta_0 + \eta_r \beta_T + x \beta_p \beta_T \sin \theta_0 + x \dot{\beta}_T \cos \theta_0 - \dot{\phi} x \dot{\beta}_T \sin \theta_0 + v \beta_T \cos \theta_0 + \mu \beta_T \cos \theta_0 \cos \psi - \mu \beta_T \dot{\phi} \sin \theta_0 \cos \psi \quad (24)$$

The velocity components at a blade section in the blade deformed frame due to hub motion are:

$$\frac{U_{R_f}}{\Omega R} = (\dot{x}_F - \dot{\alpha}_s h - y_{CG} \dot{\psi}_s) \cos \psi + (\dot{y}_F + \dot{\psi}_s h + x_{CG} \dot{\psi}_s) \sin \psi \quad (25)$$

$$\frac{U_{T_f}}{\Omega R} = (\dot{x}_F - \dot{\alpha}_s h - y_{CG} \dot{\psi}_s) \sin \psi \cos \theta_0 + (\dot{y}_F + \dot{\psi}_s h + x_{CG} \dot{\psi}_s) \cos \psi \cos \theta_0 + \sin \theta_0 (\dot{z}_F - \dot{\phi}_s x \sin \psi + \dot{\alpha}_s x \cos \psi + x_{cg} \dot{\alpha}_s - y_{cg} \dot{\phi}_s) + x \dot{\psi}_s \cos \theta_0 \quad (26)$$

$$\frac{U_{P_f}}{\Omega R} = \sin \theta_0 ((\dot{x}_F - \dot{\alpha}_s h + y_{CG} \dot{\psi}_s) \sin \psi - (\dot{y}_F + \dot{\psi}_s h + x_{CG} \dot{\psi}_s) \cos \psi) + \cos \theta_0 (\dot{z}_F - \dot{\phi}_s x \sin \psi + x \dot{\alpha}_s \cos \psi + x_{cg} \dot{\alpha}_s - y_{cg} \dot{\phi}_s) \quad (27)$$

## Fuselage Modeling

The elastic-line NASTRAN model of the AH-1G helicopter [18] was used in the coupled rotor/fuselage vibration analysis. Shaft and main rotor pylon are not considered in the current analysis. The fuselage is discretized as an elastic beam using the same 15 degree-of-freedom beam element as that used for the rotor blade. The rotor shaft is assumed to be rigidly attached to the fuselage. Therefore, the 3 translational (axial, vertical, lateral) and 3 rotational (pitch, roll, yaw) fuselage motions at the node adjacent to the shaft have a direct effect on the blade dynamics.

## Coupled Rotor/Fuselage Equations

The equation of motion for the teetering degree of freedom of a two-bladed rotor is obtained from the equilibrium of the flap moment about the teeter hinge. Blade response equations, teetering motion

equation, and fuselage response equations are solved simultaneously. To reduce computational time, the finite element equations are transformed into the normal mode space. Because the fuselage is in the fixed frame, the analysis is carried out in the fixed frame by transforming rotor equations using the multiblade coordinate transformation. To avoid singularity of the system, fuselage rigid body motion terms are moved to the right hand side of the equations. The final equations are as follows

$$\begin{aligned} & \begin{bmatrix} M_{rr} & M_{rt} & M_{rf_e} \\ M_{rt} & M_{tt} & M_{tf_e} \\ M_{fr} & M_{ft} & M_{ff_e} \end{bmatrix} \begin{Bmatrix} \ddot{\xi} \\ \ddot{\beta}_G \\ \ddot{p}_{f_e} \end{Bmatrix} \\ & + \begin{bmatrix} C_{rr} & C_{rt} & C_{rf_e} \\ C_{rt} & C_{tt} & C_{tf_e} \\ C_{fr} & C_{ft} & C_{ff_e} \end{bmatrix} \begin{Bmatrix} \dot{\xi} \\ \dot{\beta}_G \\ \dot{p}_{f_e} \end{Bmatrix} \\ & + \begin{bmatrix} K_{rr} & K_{rt} & K_{rf_e} \\ K_{rt} & K_{tt} & K_{tf_e} \\ K_{fr} & K_{ft} & K_{ff_e} \end{bmatrix} \begin{Bmatrix} \xi \\ \beta_G \\ p_{f_e} \end{Bmatrix} \\ & = \begin{Bmatrix} F_{rr} - M_{rf_e} \ddot{p}_{f_e} - C_{rf_e} \dot{p}_{f_e} \\ F_{tt} - M_{tf_e} \ddot{p}_{f_e} - C_{tf_e} \dot{p}_{f_e} \\ F_{ff_e} - C_{ff_e} \dot{p}_{f_e} \end{Bmatrix} \quad (28) \end{aligned}$$

where subscripts r, t, and f are rotor, teetering motion, and fuselage respectively.

The coupled rotor/fuselage equations are nonlinear, periodic, ordinary differential equations. A temporal finite element method is used to discretize the temporal dependence of the rotor/fuselage equations. Both blade and fuselage displacement in the fixed frame are transformed to the temporal nodal displacement using temporal shape functions. Because periodic blade forces are transmitted to the fuselage, the response of the fuselage is also periodic. Therefore, periodic boundary conditions are applied to the fuselage response as well as the blade response.

## Hub Loads

The sectional inertial force vector acting at a blade section is

$$F^I = - \int \int \rho_s \ddot{a} \, d\eta \, d\xi \quad (29)$$

where  $F^I = [L_u^I, L_v^I, L_w^I]^T$ , and  $L_u^I, L_v^I$ , and  $L_w^I$  are the distributed inertial forces acting respectively along the  $x, y$ , and  $z$  axes attached to the undeformed blade;  $\rho_s$  is the blade mass density;  $\bar{a}$  is the blade acceleration relative to an inertial frame.

The inertial component for the blade pitching moment about the deformed elastic axis is

$$\begin{aligned} M^I &= - \int \int s \times \bar{a} d\eta d\zeta \\ &= M_u^I \hat{i} + M_v^I \hat{j} + M_w^I \hat{k} \end{aligned} \quad (30)$$

where the moment arm,  $s$ , can be expressed as

$$\begin{aligned} s &= -[v'(y_1 - v) + w'(z_1 - w)]\hat{i} \\ &\quad + (y_1 - v)\hat{j} + (z_1 - w)\hat{k} \end{aligned} \quad (31)$$

The acceleration at point P on the blade is

$$\begin{aligned} \bar{a} &= \ddot{x}_1 \hat{i} + \ddot{y}_1 \hat{j} + \ddot{z}_1 \hat{k} + \dot{\bar{\omega}}_b \times \bar{r}_b \\ &\quad + 2\bar{\omega}_b \times (\dot{x}_1 \hat{i} + \dot{y}_1 \hat{j} + \dot{z}_1 \hat{k}) \\ &\quad + \bar{\omega}_b \times (\bar{\omega}_b \times \bar{r}_b) \\ &\quad + \dot{\bar{\omega}}_f \times \bar{r}_h + \bar{\omega}_f \times (\bar{\omega}_f \times \bar{r}_h) \\ &\quad + \ddot{x}_F \hat{I}_F^G + \ddot{y}_F \hat{J}_F^G + \ddot{z}_F \hat{K}_F^G \end{aligned} \quad (32)$$

where

$$\begin{aligned} \dot{\bar{\omega}}_b &= (-\ddot{\phi}_s - \dot{\alpha}_s \Omega) \hat{I}_I + (-\dot{\alpha}_s + \dot{\phi}_s \Omega) \hat{J}_I \\ &\quad + \ddot{\psi}_s \hat{K}_I + \Omega \hat{K}_I \end{aligned} \quad (33)$$

$$\dot{\bar{\omega}}_f = -\ddot{\phi}_s \hat{I}_I - \dot{\alpha}_s \hat{J}_I + \ddot{\psi}_s \hat{K}_I \quad (34)$$

The resultant blade section inertial loads induced by teetering and fuselage motions are:

$$\begin{aligned} L_u^I &= -m[-2\dot{\beta}_T \dot{w} + w\beta_T + 2x\beta_p \beta_T \\ &\quad + \ddot{x}_F \cos \psi + \ddot{y}_F \sin \psi \\ &\quad - h\ddot{\alpha}_s \cos \psi + h\ddot{\phi}_s \sin \psi - 2x\ddot{\psi}_s \\ &\quad + (x_{CG} \sin \psi - y_{CG} \cos \psi) \ddot{\psi}_s] \end{aligned} \quad (35)$$

$$\begin{aligned} L_v^I &= -m[-2w\dot{\beta}_T - 2x\dot{\beta}_T(\beta_p + \beta_T) - 2\beta_T \dot{w} \\ &\quad + \ddot{y}_F \cos \psi - \ddot{x}_F \sin \psi \\ &\quad + h\ddot{\alpha}_s \sin \psi + h\ddot{\phi}_s \cos \psi \\ &\quad + (x + x_{CG} \cos \psi + y_{CG} \sin \psi) \ddot{\psi}_s] \end{aligned} \quad (36)$$

$$\begin{aligned} L_w^I &= -m[x\dot{\beta}_T + x\beta_T + \ddot{z}_F \\ &\quad + (x \cos \psi + x_{CG}) \ddot{\alpha}_s \\ &\quad - 2x\ddot{\alpha}_s \sin \psi - (x \sin \psi + y_{CG}) \ddot{\phi}_s \\ &\quad - 2x\ddot{\phi}_s \cos \psi] \end{aligned} \quad (37)$$

Steady and vibratory components of blade loads (rotating frame) that include fuselage motion effects are calculated using the force summation

Table 1 Blade Properties

Number of blade	2
Rotor radius	22(ft)
chord	27(in)
Rotor speed	324(RPM)
Lock number	5.078
Precone angle	2.75(deg)
Twist at tip	-10(deg)
Control system spring rate	396000(in-lb/rad)
Pitch link moment arm	9.067(in)
Lift curve slope	6.159

method. Fixed frame hub loads are calculated by summing the contributions from individual blades.

In a typical aeromechanics analysis, only constant hub loads are satisfied in the vehicle trim solution. For a level flight condition, the fuselage is assumed to be stationary, and the harmonic components of rotor hub forces are not balanced with fuselage dynamic forces. However, in the vibration analysis, vibratory hub loads are used to calculate velocities and accelerations of the fuselage, and therefore their equilibrium with the fuselage dynamic forces is necessary. A coupled trim procedure is carried out to solve the blade response, fuselage elastic response, fuselage rigid response, pilot control setting, and vehicle orientation simultaneously. In this analysis, impedance matching is inherently satisfied.

## Results and Discussion

The two-bladed teetering rotor of the AH-1G helicopter is used in this analysis. Detailed flight conditions and helicopter properties can be found in reference [19]. The description of the baseline configuration is given in Table 1. The blade is discretized into 13 beam elements with each element consisting of fifteen degrees of freedom and its mass and stiffness distributions are in Table 2. Coupled rotor/fuselage vibration results calculated by the present analysis are compared with measured values. Its collective mode (hingeless boundary condition) natural frequencies are given in Table 3 and compared with those used by C81 program. Flap frequencies are quite well matched with data, but lag and torsion frequencies of present analysis are larger than those used by C81 program.

Each fuselage element is assumed to be an elastic beam undergoing vertical and lateral bending, elastic twist and axial deflections. The rotor

Table 2 Blade Mass and Stiffness Distribution

	Length	Mass	$EI_z$	$EI_y$ $\times 10^{-1}$	GJ $\times 10^{-2}$
1	0.01326	7.3164	0.3049	0.2102	0.2194
2	0.02841	2.2604	0.2550	0.0057	0.2194
3	0.01174	6.3769	0.5176	0.2075	0.2194
4	0.08864	5.6266	0.1039	0.1818	0.2122
5	0.01326	6.3257	0.0275	0.4876	0.408
6	0.04470	3.6441	0.5017	0.2486	0.5156
7	0.10871	0.7562	0.2527	0.0454	0.4105
8	0.19129	0.7344	0.2481	0.0306	0.2816
9	0.09015	0.6996	0.2137	0.0244	0.2084
10	0.10985	0.9551	0.1888	0.0249	0.206
11	0.10417	1.0189	0.1615	0.0241	0.206
12	0.09773	1.0847	0.1617	0.0257	0.206
13	0.09811	1.0368	0.1631	0.0245	0.206

Table 3 Blade Natural Frequencies

Present Analysis (/rev)	C81 input [20] (/rev)
flap 1	1.04
flap 2	2.79
flap 3	4.81
lag	1.43
torsion	2.58

Table 4 Fuselage Natural Frequencies

Present Analysis (/rev)	NASTRAN [18] Analysis (/rev)
vertical	1.44
bending	3.16
	5.1
lateral	1.36
bending	3.07

is connected to the body at node 11 through a rigid shaft. Because the present model does not consider the main rotor pylon, only fuselage natural frequencies are given in Table 4 and compared with NASTRAN predictions. The close agreement between the two sets of values can be seen.

The coupled rotor/fuselage equations are solved in straight and level flight condition to satisfy three force and three moment vehicle equilibrium equations. A finite element method in time is used to solve the periodic equations and a pseudo-implicit free wake model is used to determine inflow distribution. A coupled trim solution is obtained for different advance ratios. A comparison of calculated rotor control angles with flight test data is shown in Fig. 3 The general

trends are good, but the analysis underpredicts collective and longitudinal cyclic angles

Blade torsional moment, chord bending moment, and beam bending moment are presented in Figs. 4 through 9 as a function of blade radius position at low and high advance ratios and compared with flight test data.

Three different analysis options are used for each case. First is the hub-fixed model, second is the rigid body model, and third is the elastic line body model. The first case represents the hub fixed condition and the feedback of fuselage motion is neglected. For the second case, only rigid body motions of the fuselage are included. For this, three translations and three angular hub motions are included. For the third case, elastic motions of the fuselage are included to determine blade loads.

At an advance ratio of 0.15, calculated torsional moments show the expected trend with the test data, but overpredict 1/rev harmonics near the root and underpredict 2/rev and 3/rev harmonics(Fig. 4). The fuselage feedback effect is small in the torsional moment. Estimated chord bending moments show good agreement with test data(Fig. 5). Fuselage feedback motion reduces all harmonic components along the blade span and improves correlation between the analysis and flight test data. The effect of fuselage flexibility is small. Beam bending moments overpredict all harmonic components along the blade span(Fig. 6). Fuselage feedback motion increases, especially 2/rev and 3/rev harmonics, and deteriorates the estimation.

At an advance ratio of 0.32, the fuselage feedback motion effect slightly improves 1/rev and 3/rev torsional moments estimation(Fig. 7). Even at this high advance ratio, the effect of fuselage flexibility is negligible. Chord bending moments are overpredicted, especially the 1/rev harmonic component(Fig. 8). The difference is bigger near the root. Predicted beam bending moments show the same overprediction as that at the low advance ratio(Fig. 9). The difference between the present analysis and the test data for the 3/rev harmonic component is significant. A further investigation should be carried out to improve prediction of this moment.

Figs. 10 through 12 show nondimensionalized 2/rev hub forces at different advance ratios. Fuselage feedback motion decreases longitudinal and lateral hub forces and increases vertical hub forces. The effect of elastic body modes is small in the longitudinal and lateral hub forces and large in the vertical hub forces.

Figs. 13 and 14 show 2/rev and 4/rev vertical acceleration at the pilot seat. Estimated 2/rev and 4/rev vertical acceleration results show good correlation with the flight test data. Figs. 15 and 16 respectively show 2/rev and 4/rev lateral acceleration at the pilot seat. Test data for this condition show almost constant vibration levels at different advance ratios. Calculated 2/rev lateral acceleration level increases with advance ratios and overpredicts at all advance ratios. The 4/rev vibration level is well matched with test data at low advance ratios, but overpredicts at high advance ratios.

### Conclusions

A comprehensive vibration analysis of a coupled rotor/fuselage system for a two-bladed teetering rotor using finite element methods in space and time is developed. Elastic fuselage modeling capability is incorporated with elastic rotor analysis.

From the validation study, the following conclusions are drawn.

1. Correlation of fuselage frequencies with the NASTRAN elastic line model of the AH-1G helicopter shows good agreement in the vertical and lateral directions.
2. In general, there is a fair agreement for rotor controls. Predicted collective and longitudinal cyclic pitch angles respectively vary by 2 to 3 degrees from measured values.
3. Comparison between the calculated blade torsional and chord bending moments and measured data shows relatively good agreement, but calculated beam bending moments significantly overpredict measured data and needs to be investigated further.
4. Estimated 2/rev and 4/rev vertical acceleration at pilot seat shows good correlation with the flight test data.
5. Measured 2/rev lateral acceleration levels at the pilot seat is overpredicted at all advance ratios. The 4/rev lateral acceleration level shows good agreement at low advance ratios, but overpredicts at high advance ratios.

Parametric studies will be carried out to investigate the sensitivity of different design parameters and modeling refinements on the prediction of blade loads and vibration.

### Acknowledgments

This work was supported by the National Rotorcraft Technology Center under Grant No. NCC 2944; Technical monitor Dr. Yung Yu. The authors would like to acknowledge many useful discussions with Mr. John Corrigan, Bell Helicopter Textron.

### References

- [1] Reichert, G., "Helicopter Vibration Control-A Survey", *Vertica*, Vol. 5, No. 1, 1981, pp. 1-20.
- [2] Loewy G. R., "Helicopter Vibrations: A Technological Perspective", *Journal of the American Helicopter Society*, Vol. 29, No. 4, October 1984, pp. 4-30
- [3] Kvaternik, R. G., Bartlett, Jr. F. D., and Cline, J. H., "A Summary of Recent NASA/Army Contributions to Rotorcraft Vibration and Structural Dynamics Technology", *NASA CP-2495*, February 1988.
- [4] Staley, J. A. and Sciarra, J. J., "Coupled Rotor/Airframe Vibration Prediction Methods", *Rotorcraft Dynamics - NASA SP-352*, 1974, pp. 81-90
- [5] Hohnemeser, K. H. and Yin, S. K., "The Role of Rotor Impedance in the Vibration Analysis of Rotorcraft", *Vertica*, Vol 3, 1979, pp. 187-204.
- [6] Hsu, T. K. and Peters, D. A., "Coupled Rotor/Airframe Vibration Analysis by a Combined Harmonic-Balance Impedance Matching Method", 36th Annual National Forum of the American Helicopter Society, Washington D.C., May 1980.
- [7] Kunz, D. L., "A Nonlinear Response Analysis for Coupled Rotor-Fuselage System", American Helicopter Society Specialists' Meeting on Helicopter Vibration Technology for the Jet Smooth Ride, Hatford, Nov. 1981.
- [8] Rutkowski, J. M., "The Vibration Characteristics of a Coupled Helicopter Rotor-Fuselage by a Finite Element Analysis", *NASA TP-2118*, January 1983.
- [9] Gable, R. and Sankewitsch, V., "Rotor-Fuselage Coupling by Impedance", 42nd Annual National Forum of the American

- [10] Warmbrodt, W. and Friedmann, P. P., "Formulation of Coupled Rotor/Fuselage Equations of Motion", *Vertica*, Vol. 3, No. 3/4, 1979, pp. 245-271.
- [11] Bir, G. and Chopra, I., "Prediction of Blade Stresses due to Gust Loading", *Vertica*, Vol. 10, No. 3/4, 1986, pp. 353-377
- [12] Vellaichamy, S. and Chopra, I., "Effect of Modeling Techniques in the Coupled Rotor-Body Vibration Analysis", Proceedings of the 34th Structures, Structural Dynamics and Materials Conference and Adaptive Structures Forum, LaJolla, April 1993.
- [13] Chiu, T. and Friedmann, P. P., "A Coupled Helicopter Rotor/Fuselage Aeroelastic Response Model for ACSR", Proceedings of the 36th Structures, Structural Dynamics and Materials Conference and Adaptive Structures Forum, New Orleans, April 1995.
- [14] Chiu, T. and Friedmann, P. P., "ACSR System for Vibration Suppression in Coupled Helicopter Rotor/Flexible Fuselage Model", Proceedings of the 37th Structures, Structural Dynamics and Materials Conference and Adaptive Structures Forum, Salt Lake City, April 1996.
- [15] Yeo, H. and Chopra, I., "Modeling Issues Related to Vibration Prediction of a Coupled Rotor/Fuselage System", Proceedings of the 38th Structures, Structural Dynamics and Materials Conference and Adaptive Structures Forum, Kissimmee, FL, April 1997.
- [16] Bagai, A. and Leishman, J. G., "Rotor Free-Wake Modeling using a Pseudo-Implicit Relaxation Algorithm", AIAA paper No. 94-1918, AIAA 12th Applied Aerodynamics Conference, Colorado Springs, Colorado, June 1994.
- [17] Leishman, J. G., "Validation of Approximate Indicial Aerodynamic Functions for Two-Dimensional Subsonic Flow", *Journal of Aircraft*, Vol. 25, No. 10, October 1988.
- [18] Hanson, H. W., "Investigation of Vibration Reduction Through Structural Optimization", USAAVRADCOTR-80-D-13, June 1980.
- [19] Dompka, R. V. and Cronkhite, J. D., "Summary of AH-1G Flight Vibration Data for Validation of Coupled Rotor-Fuselage Analyses", *NASA CR 178160*, November 1986.
- [20] Dompka, R. V. and Corrigan, J. J., "AH-1G Flight Vibration Correlation Using NASTRAN and the C81 Rotor/Fuselage Coupled Analysis", 42nd Annual AHS Forum, Washington, D.C., June 1986.

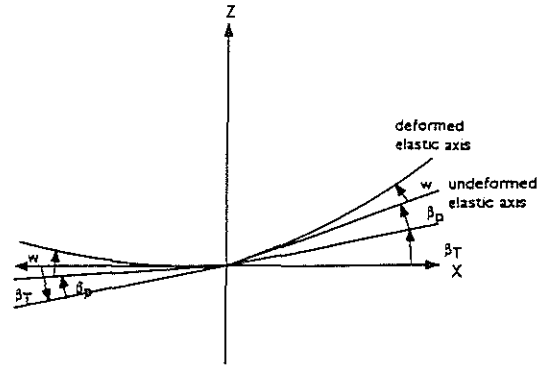


Fig. 1 Coordinate system of a teetering rotor

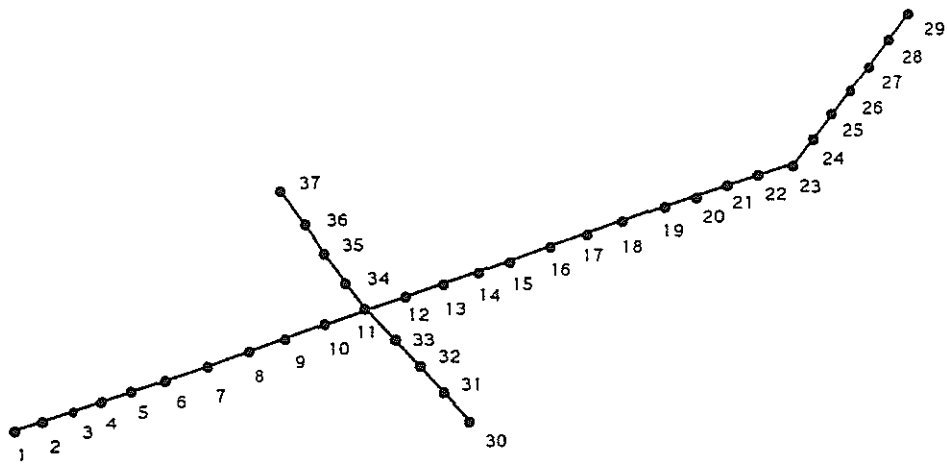


Fig. 2 Finite Element Modeling of a Fuselage

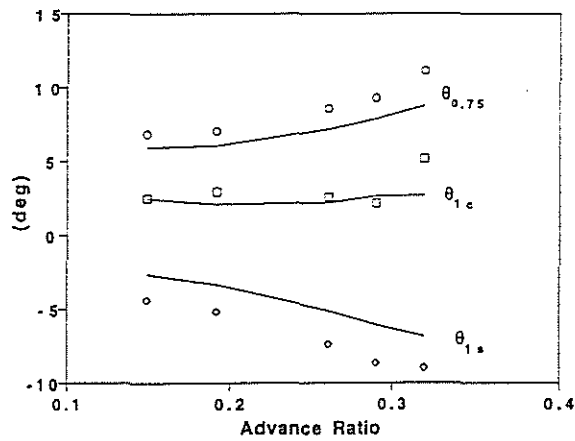


Fig. 3 Rotor Controls

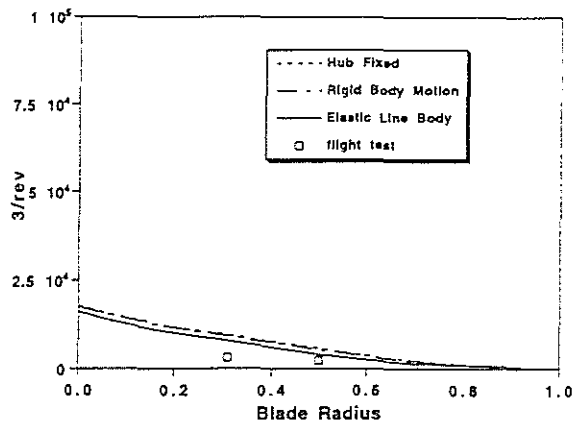
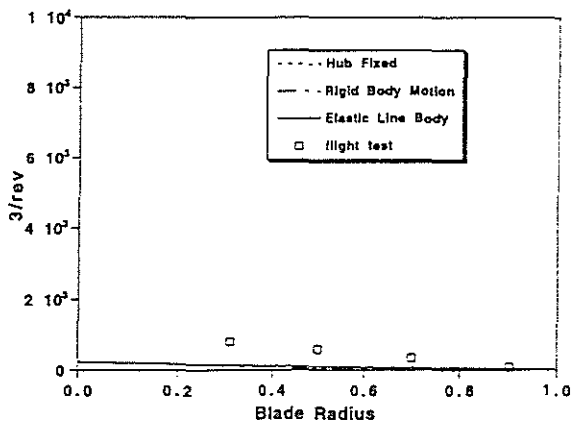
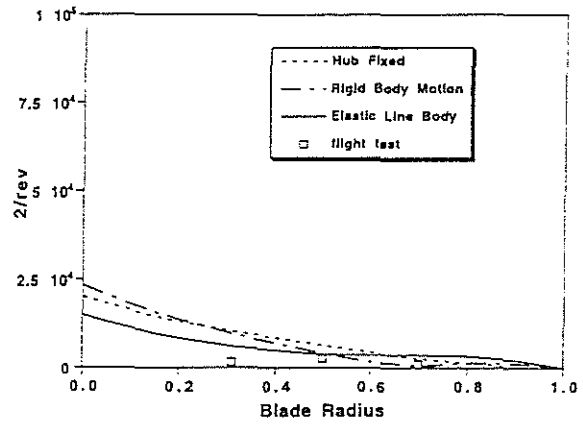
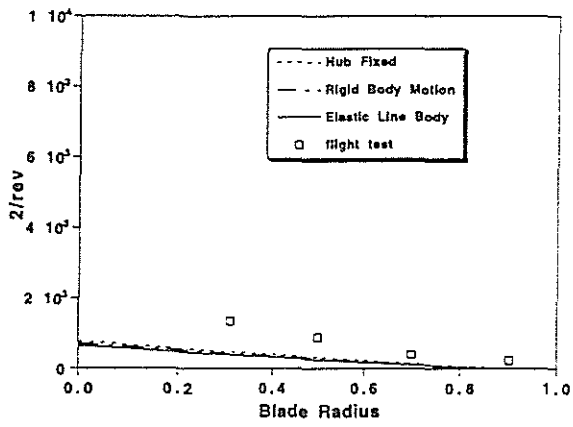
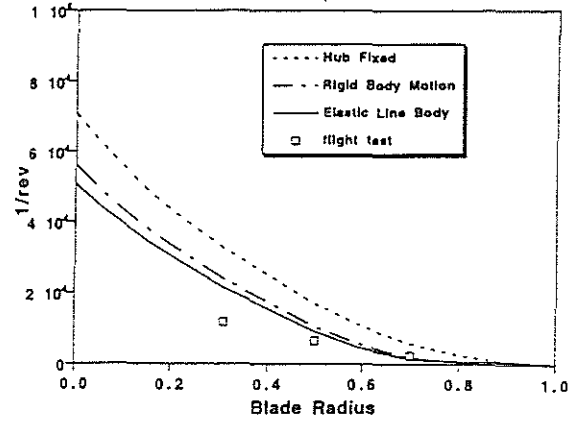
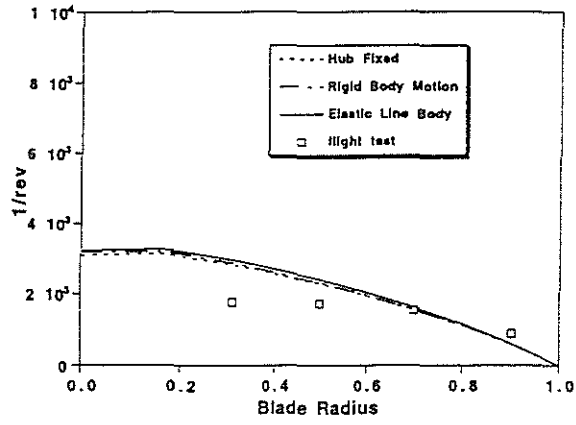


Fig. 4 Torsional moment at advance ratio 0.15

Fig. 5 Chord bending moment at advance ratio 0.15

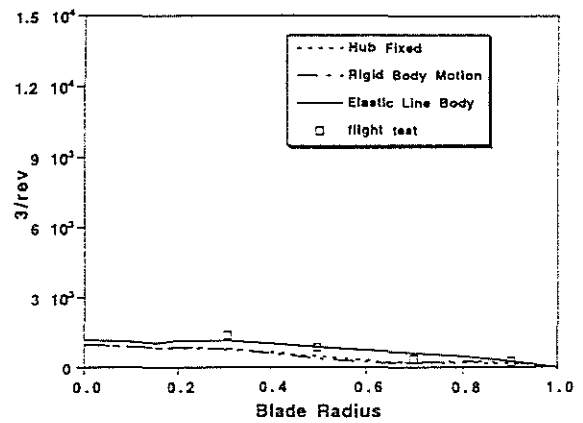
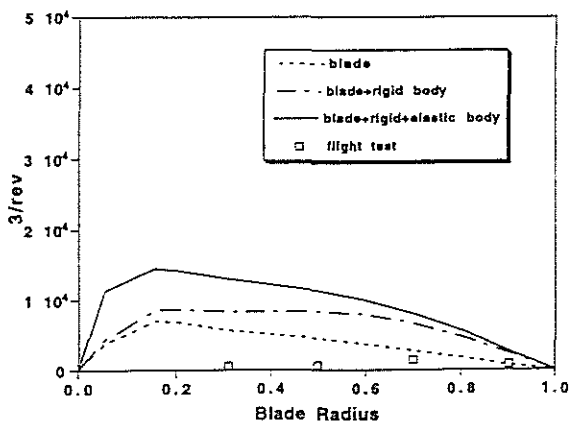
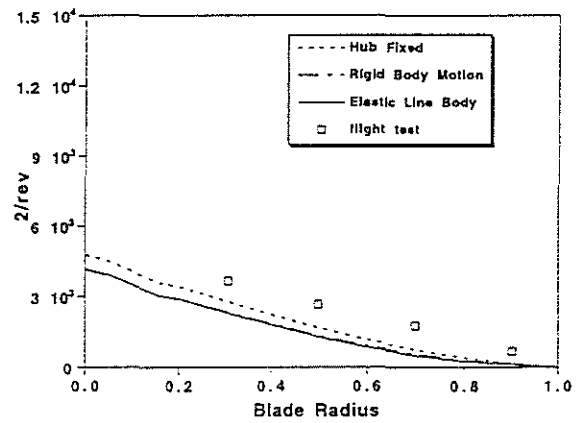
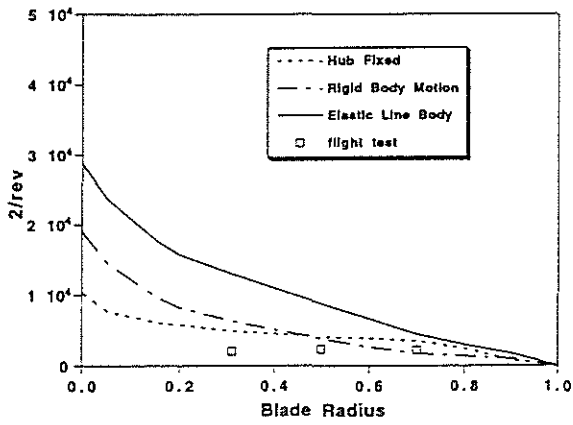
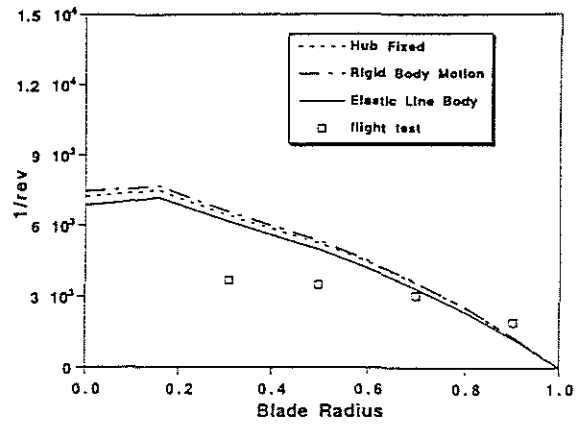
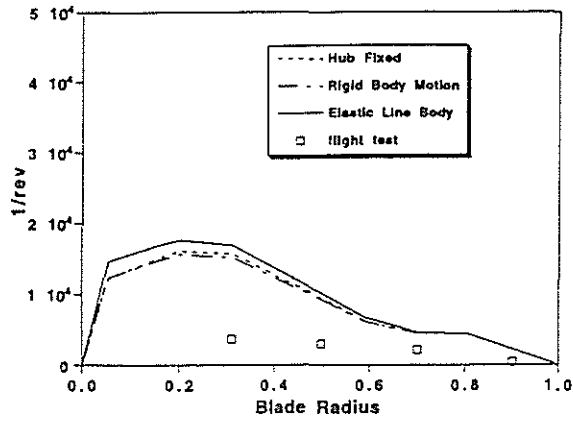


Fig. 6 Beam bending moment at advance ratio 0.15

Fig. 7 Torsional moment at advance ratio 0.32

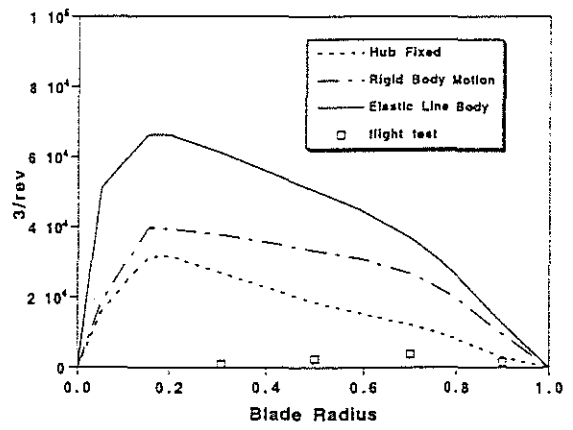
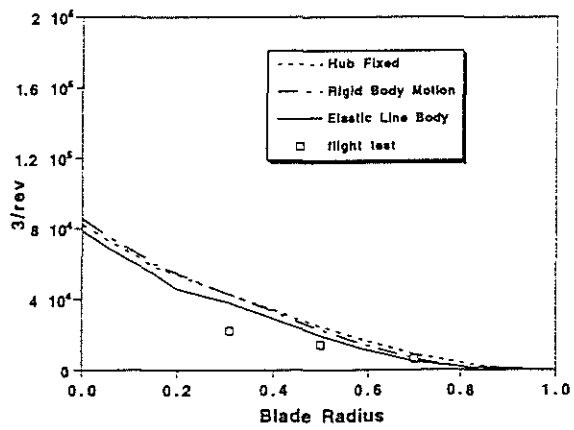
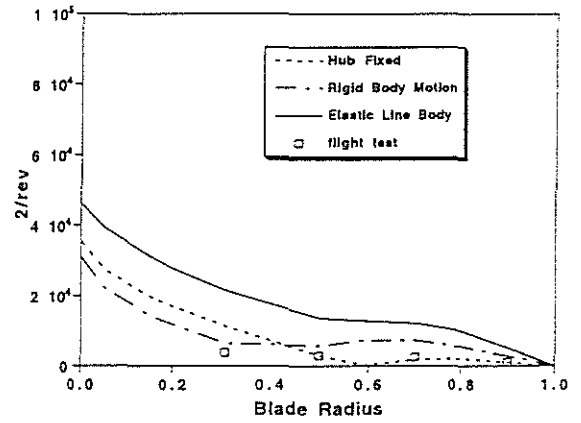
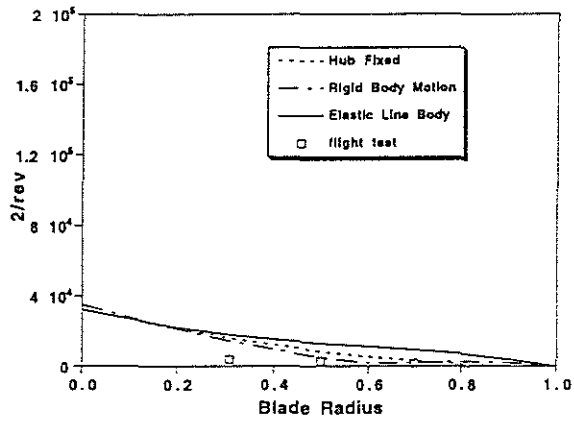
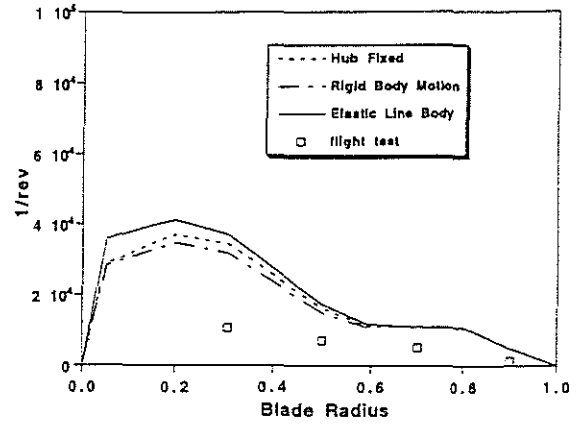
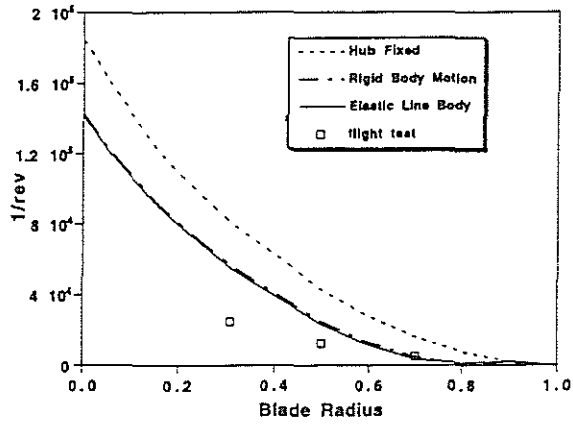


Fig. 8 Chord bending moment at advance ratio 0.32

Fig. 9 Beam bending moment at advance ratio 0.32

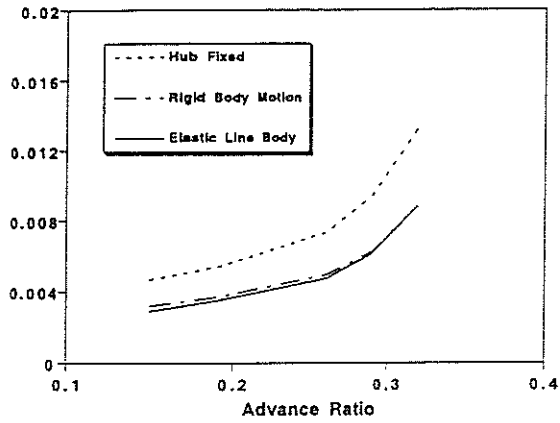


Fig. 10 2/rev longitudinal hub force

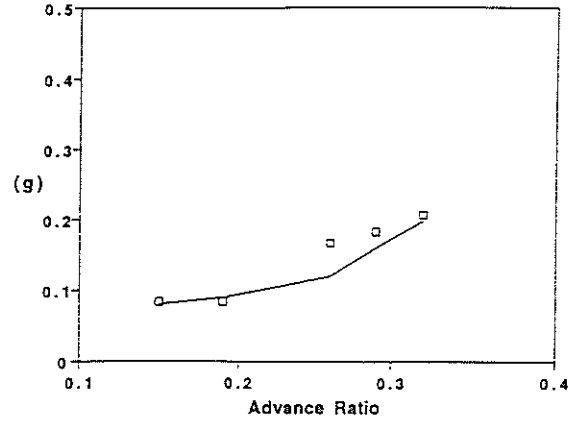


Fig. 13 2/rev vertical acceleration at pilot seat

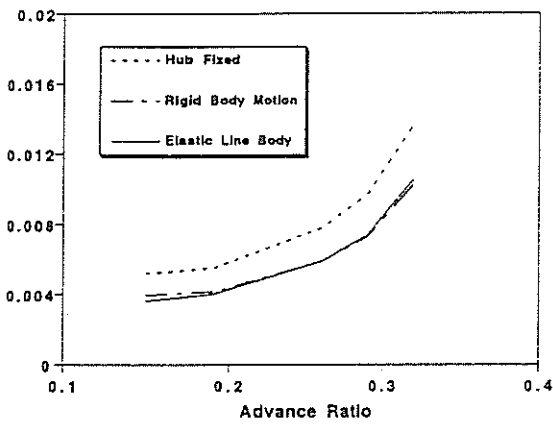


Fig. 11 2/rev lateral hub force

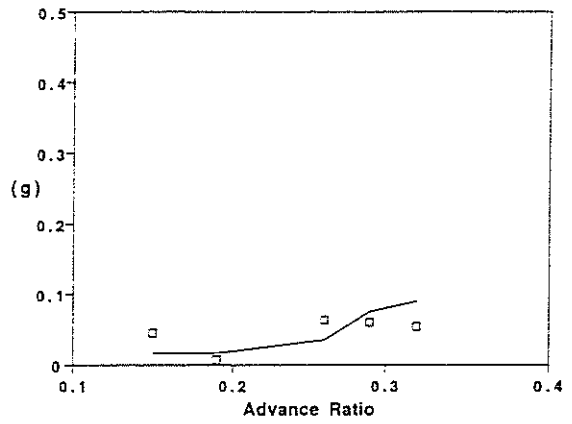


Fig. 14 4/rev vertical acceleration at pilot seat

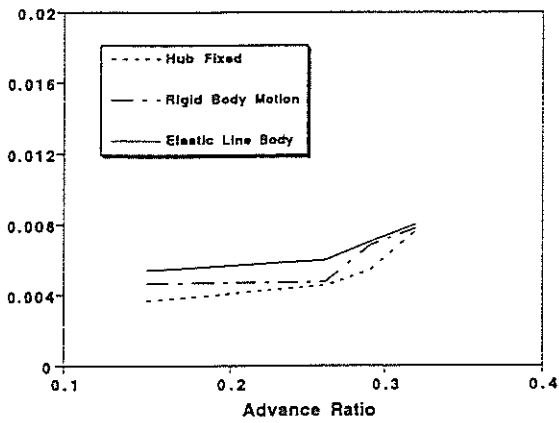


Fig. 12 2/rev vertical hub force

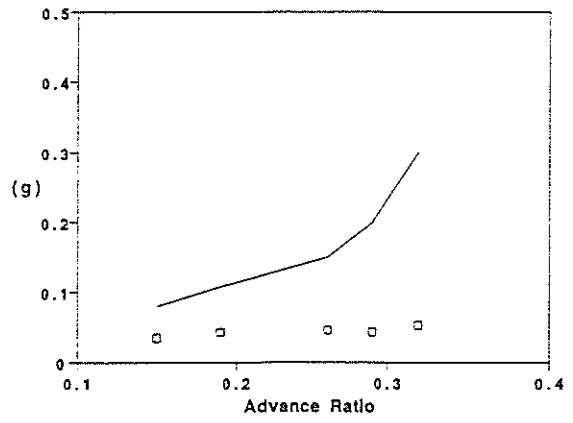


Fig. 15 2/rev lateral acceleration at pilot seat

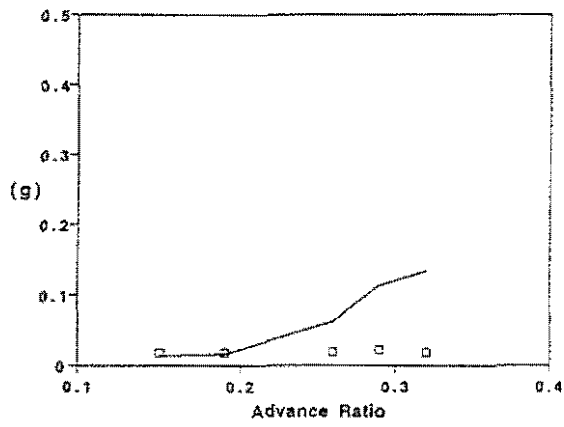


Fig. 16 4/rev lateral acceleration at pilot seat